Hydrogenation of Xylenes, Ethylbenzene, and Isopropylbenzene on Ni Nanocatalyst

R. V. Shafigulin[a], A. V. Bulanova[a] *, M. V. Kuznetsov[b] **, A. V. Safonov[b], I. P. Parkin[c], and Yu. G. Morozov[d] ***

[a] *Department of Chemistry, Samara University, Samara, 443086 Russia*
[b] *All-Russia Research Institute on Problems of Civil Defense and Emergencies, Emergency Control Ministry (EMERCOM), Moscow, 121352 Russia*
[c] *Department of Chemistry, Materials Chemistry Research Centre, University College London, London, WC1H 0AJ, United Kingdom*
[d] *Merzhanov Institute of Structural Macrokinetics and Material Science (ISMAN), Russian Academy of Sciences, Chernogolovka, 142432 Russia*

* av.bul@yandex.ru
** maxim1968@mail.ru
*** morozov@ism.ac.ru

Received November 8, 2021; revised November 24, 2021; accepted

Abstract—Kinetic and thermodynamic parameters of the catalysts containing 15% of the Ni nanoparticles prepared by levitation-jet method in hydrogenation of xylenes, ethylbenzene, and isopropylbenzene were studied using a laboratory-made chromatographic setup. At relatively low hydrogen pressure (2 atm) and temperatures of 423–493 K, our catalysts provide a high extent of conversion of the compounds studied and selectivity with respect to *p*-xylene.

Keywords: Ni nanoparticles, heterogeneous catalysis, hydrogenation, aromatic hydrocarbons

1. INTRODUCTION

In a view of their specific structural, physicochemical, and catalytic parameters, metal nanoparticles find application in petrochemical industry [1–3] as catalysts for hydrogenation of unsaturated and aromatic hydrocarbons [4, 5]. In this context, a search for new effective, selective, and environment-friendly catalysts is of current importance and significance [6, 7].

In this communication, we report on the catalytic behavior of the composite containing 15% Ni nanoparticles prepared by levitation-jet method in hydrogenation of xylenes, ethylbenzene, and isopropylbenzene.

2. EXPERIMENTAL

The nickel nanoparticles with a size of 50–200 nm were home-made at ISMAN by using a levitation-jet generator [8]. The TEM image of studied Ni nanoparticles is shown at Figure 1. The catalysts used in our experiments were prepared by deposition of Ni nanoparticles in an amount of 15% onto Inerton NAW–DMCS in hexane followed by sonication before evaporation.

Catalytic hydrogenation reaction was run under steady-state conditions using the laboratory-made setup described elsewhere [3]. A 1-mL stainless steel tube was used as a reactor. A hydrocarbon in an amount of 0.5 μL was injected into the reactor in a hydrogen flow using a micro syringe. The hydrogenation reaction was run at a hydrogen pressure of 2 atm and T = 423–493 K. A hydrogen/hydrocarbon molar ratio in the reactor was kept around 18. For more details of our chromatographic experiments, see [9–11].

Based on the results of chromatographic measurements, we could determine the following kinetic parameters of hydrogenation reaction.

– Rate constant for first-order reaction

$$k = (1/t) \ln (S_0/S_t) \quad (1)$$

where S_0 is the peak area of starting hydrocarbon in a chromatogram at t = 0 and S_t is that at time t.

– Extent of conversion (κ) for a hydrocarbon

$$\kappa = 1 - S_t/S_0 \quad (2)$$

– Pre-exponential factor A was derived from the Arrhenius equation written in the form [11]:

$$\ln k = \ln A - E^{\neq}/RT \quad (3)$$

– Entropy of activation $\Delta S_p^{\neq}$ was calculated as

$$\Delta S_p^{\neq} = R \ln\left(\frac{Ah}{\chi k_B T e^x}\right) + (1-x) R \ln(RT) \quad (4)$$

where R is absolute gas constant, k_B is the Boltzmann constant, h is the Planck constant, x is a reaction order, and χ is a transmission coefficient.

3. RESULTS AND DISCUSSION

3.1. Hydrogenation of Xylenes

Figure 2 presents the chromatograms of reaction mixture for the hydrogenation of *p*-xylene. Chromatogram (*a*) was obtained using katharometer as a detector while chromatogram (b), a mass-spectrometric detection system. Similar chromatograms were recorded for the hydrogenation of *o*- and *m*-xylenes.

Using the chromatograms, taken at some certain *t* values and Eq. (1), we could plot the linear dependences of ln *S* on *t* (Fig. 3) for all three xylenes. Rate constants *k* derived from these plots are collected in Table 1.

We also theoretically estimated the activation energy and formation entropy for transition complex in the process of hydrogenation. The results are presented in Table 2. Figure 4 represents the extent of xylene's conversion κ at $T = 423$ K as a function of *t*.

Therefore, our results suggests that an isomeric structure of xylenes markedly affects a magnitude of κ and $E^{\neq}$. In case of *p*-xylene, a key role in the formation of activation complex is played by the entropy factor, while in case of *o*- and *m*-xylene, by the energy factor. It implies that, in simultaneous hydrogenation of all three xylenes, the reaction is most selective for *p*-xylene. Hence, it is *p*-xylene that can be separated from its isomers in some certain conditions.

3.2. Hydrogenation of ethylbenzene and isoprpopylbenzene

Figure 5 represents the chromatograms of reaction mixture for the hydrogenation of ethylbenzene and isopropylbenzene. The rate constants *k* derived from these results are presented in Table 3. The results of our calculations are presented in Table 4, Fig. 6, and Fig. 7. The above results allowed us to conclude that: (a) activation energy plays a key role in the formation of activation complex and (b) the hydrogenation of ethylbenzene and isopropylbenzene proceeds by close mechanisms.

CONCLUSIONS

Our catalysts containing Ni nanoparticles prepared by levitation-jet method may turn interesting to those engaged in R & D of new catalytic systems for hydrogenation of aromatic hydrocarbons.

REFERENCES

1. Gao, L., Kojima, K., and Nagashima, H., Transition metal nanoparticles stabilized by ammonium salts of hyperbranched polystyrene: Effect of metals on catalysis of the biphasic hydrogenation of alkenes and arenes, *Tetrahedron*, 2015, vol. 71, no. 37, pp. 6414–6423. http://dx.doi.org/10.1016/j.tet.2015.04.081

2. Mallikarjuna, K. and Kim, H., Synthesis and characterization of highly active Cu/Pd bimetallic nanostructures, *Coll. Surf. A: Physicochem. Eng. Aspects*, 2017, vol. 535, pp. 194–200. https://doi.org/10.1016/j.colsurfa.2017.09.045
3. Shubina, E.G., Filimonov, N.S., Shafigulin, R.V., Bulanova, A.V., Shishkovskii, I.V., and Morozov Yu.G., Effect of size of nickel nanoparticles on hydrogenation of benzene, *Petrol. Chem*., 2017, vol. 57, no. 5, pp. 410–414. https://doi.org/10.1134/S0965544117020244
4. Giustra, Z.X., Ishibashi, J.S.A., and Liu, S.-Y., Homogeneous metal catalysis for conversion between aromatic and saturated compounds, *Coord. Chem. Rev.*, 2016, vol. 314, pp. 134–181. https://doi.org/10.1016/j.ccr.2015.11.006
5. Peyrovi, M.H., Parsafard, N., and Mohammadian, Z., Benzene selective hydrogenation over supported Ni (nano-) particle catalysts: Catalytic and kinetics studies, *Chin. J. Chem. Eng.*, 2018, vol. 26, no. 3, pp.521–528. https://doi.org/10.1016/j.cjche.2017.05.022
6. Li, F., Wang. X., Zheng, Y., and Chen, J., Influence of metallic promoters on the performance of Ni/SiO_2 catalyst in the hydrodeoxygenation of anisole, *J. Fuel Chem. Technol.*, 2018, vol. 46, no. 1, pp. 75–83. https://doi.org/10.1016/S1872-5813(18)30005-7
7. Singh, H., Glucose hydrogenation to sorbitol over unsupported mesoporous Ni/NiO catalyst, *Mol. Catal*., 2018, vol. 451, pp. 186–191. https://doi.org/10.1016/j.mcat.2018.01.010
8. Morozov, Yu.G., Belousova, O.V., Kuznetsov, M.V., Ortega, D., and Parkin, I.P., Electric field-assisted levitation-jet aerosol synthesis of Ni/NiO nanoparticles, *J. Mater. Chem.*, 2012, vol. 22, no. 22, p. 11214. https://doi.org/10.1039/c2jm31233f
9. Shishkovsky, I.V., Bulanova, A.V., and Morozov, Yu.G. Porous polycarbonate membranes with Ni and Cu nano catalytic additives fabricated by selective laser sintering, *J. Mater. Sci. Eng. B*, 2012, vol. 2, no. 12, pp. 634–639.
10. Yadrova, A.A., Shafigulin, R.V., and Bulanova, A.V., Chromatographic behavior of benzimidazole derivatives on hypercrosslinked polystyrene by reverse-phase HPLC, *J. Liq. Chromatogr. Rel. Technol.*, 2020, vol. 43, no. 13–14, pp. 482–493. https://doi.org/10.1080/10826076.2020.1734024
11. Yadrova, A.A., Grinevich, O.I., Shafigulin, R.V., and Bulanova A.V., Influence of ionic liquids' nature on chromatographic retention of benzimidazoles by RP HPLC, *J. Liq. Chromatogr. Rel. Technol.*, 2021, vol. 44, nos. 3−4, pp.127−139. https://doi.org/10.1080/10826076.2020.1858315

Translated by Yu. Scheck

Table 1. Rate constants k ($min^{-1} \times 10^3$) for hydrogenation of xylenes at 423 and 493 K

T, K	*m*-xylene	*o*-xylene	*p*-xylene
423	13.9	16.3	4.2
493	51.4	18.7	13.8

Table 2. Activation energy $E^{\neq}$ and entropy $S^{\neq}$ for the formation of transition complexes in hydrogenation of xylenes

Compound	$E^{\neq}$, kJ/mol	$-S^{\neq}$, J/mol K
m-xylene	102	17
o-xylene	11	231
p-xylene	29	197

Table 3. Rate constants k (min^{-1}) for hydrogenation of ethylbenzene and isopropylbenzene at 423 K and 443 K (x 10^3)

T, K	Ethylbenzene	Isopropypbenzene
423	6.1	8.3
493	15.2	19.9

Table 4. Activation energy $E^{\neq}$ and entropy $S^{\neq}$ for the formation of transition complexes in hydrogenation of ethylbenzene and isopropylbenzene

Compound	$E^{\neq}$, kJ/mol	$-S^{\neq}$, J/mol K
Ethylbenzene	23	211
Isopropypbenzene	26	203

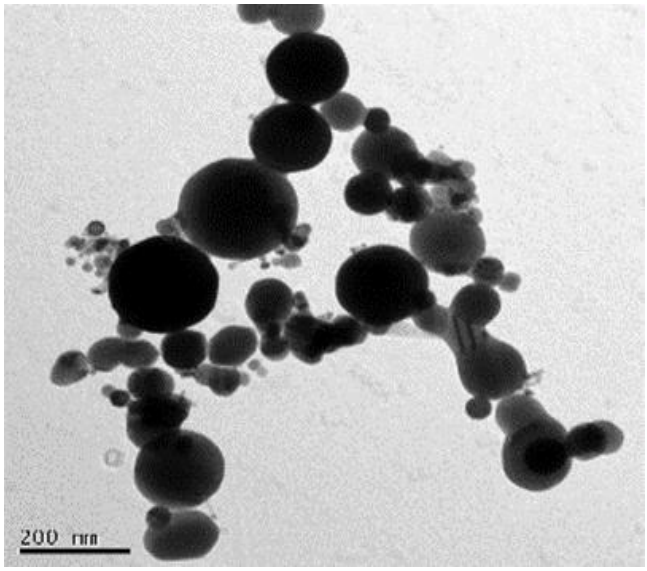

Key: 200 nm

Fig. 1. TEM image of Ni nanoparticles prepared by levitation-jet method.

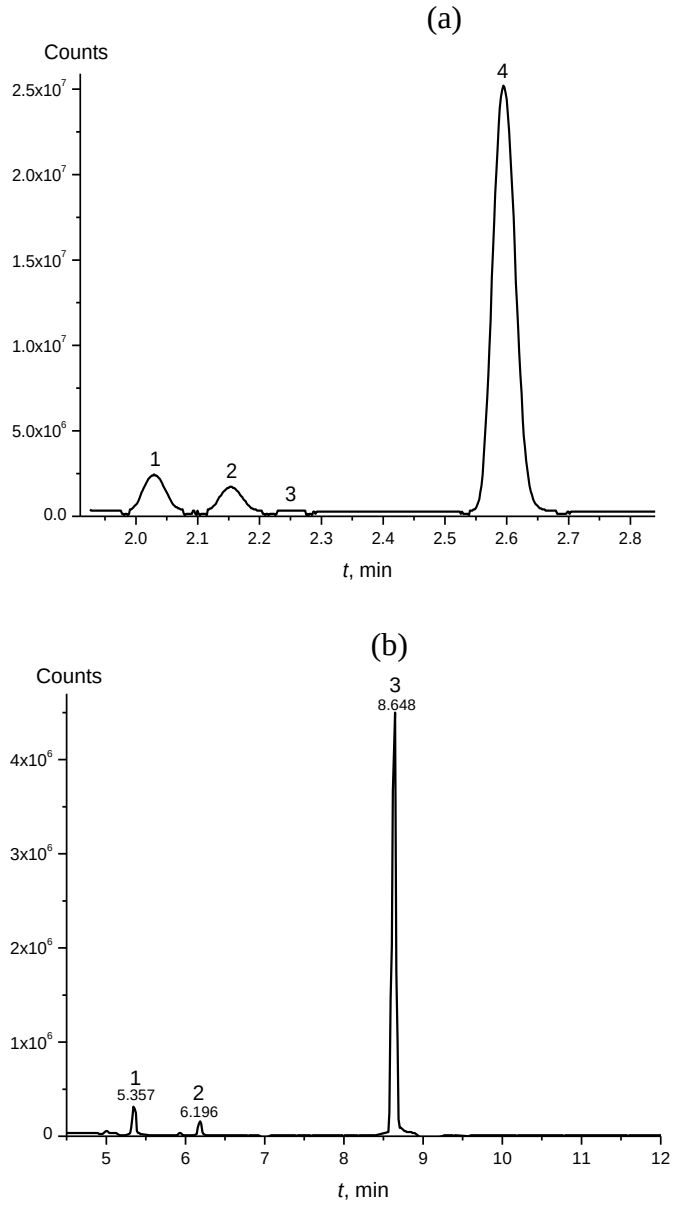

Fig. 2. Chromatogram of reaction mixture for the hydrogenation of *p*-xylene: *t* = 5 min, *T* = 423 K, *P* (H_2) = 2 atm. Peak assignments: (1) *trans*-1,4-dimethylcyclohexane, (2) *cis*-1,4- dimethylcyclohexane, (3) *p*-xylene. Chromatogram (*a*) was obtained using a katharometer as detector while chromatogram (*b*), a mass-spectrometric detection system.

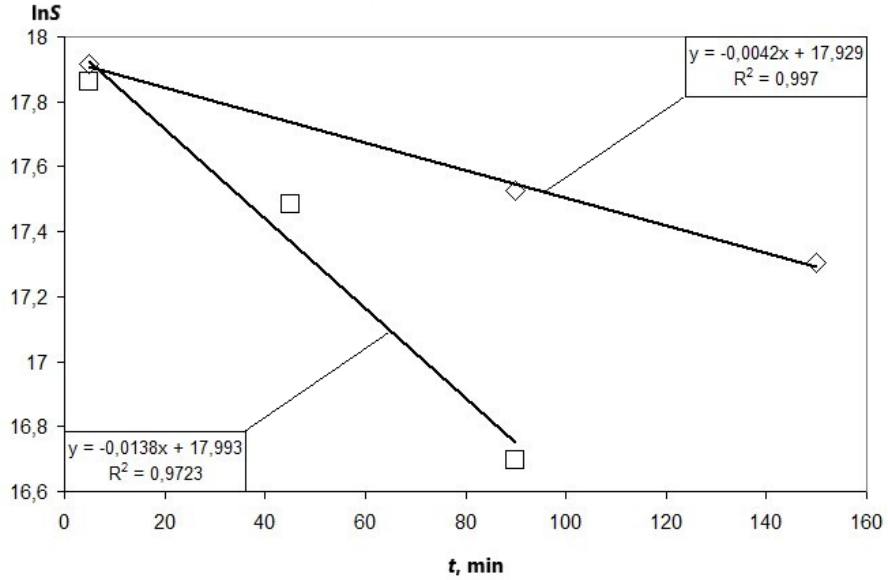

Key: ln *S* *t*, min

Fig. 3. Hydrogenation of *p*-xylene at 423 K (◊) and 493 K (□): ln *S* as a function of *t*; $P(H_2)$ = 2 atm.

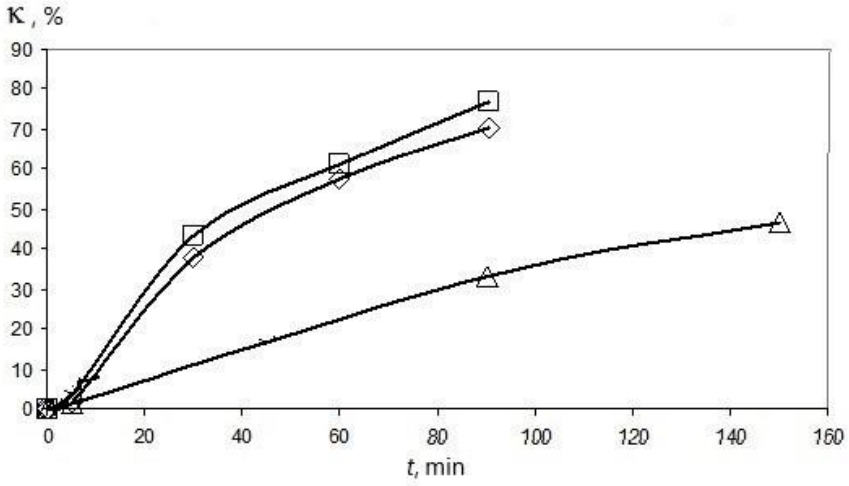

Key: κ, % *t*, min

Fig. 4. Hydrogenation of *meta*- (◊), *ortho*- (□), and *para*-xylene (Δ): extent of conversion κ as a function of *t* at T = 423 K, $P(H_2)$ = 2 atm.

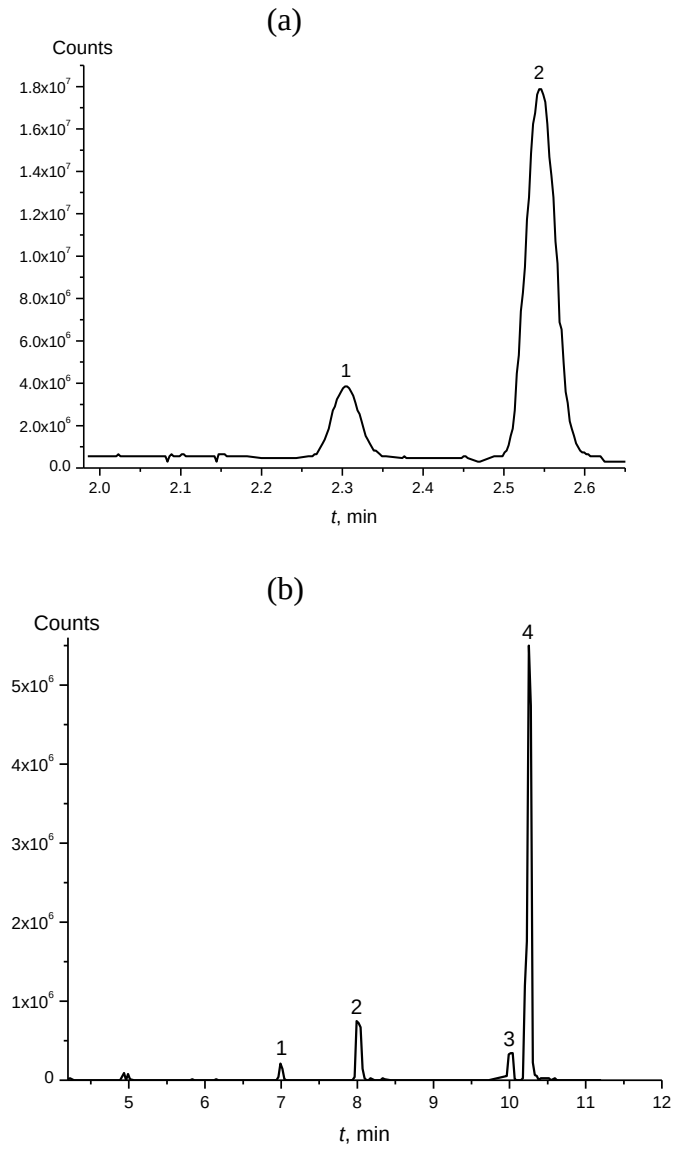

Fig. 5. Chromatograms of reaction mixture for the hydrogenation of:
(a) ethylbenzene [t = 5 min, T = 423 K, $P(H_2)$ = 2 atm]: (1) ethylcyclohexane, (2) ethylbenzene; and (b) isopropylbenzene [t = 5 min, T = 433 K, $P(H_2)$ = 2 atm]: (1) ethylcylohexane, (2) ethylbenzene, (3) isopropylcyclohexane, (4) isopropylbenzene. Chromatogram (*a*) was obtained using a katharometer as detector while chromatogram (*b*), a mass-spectrometric detection system.

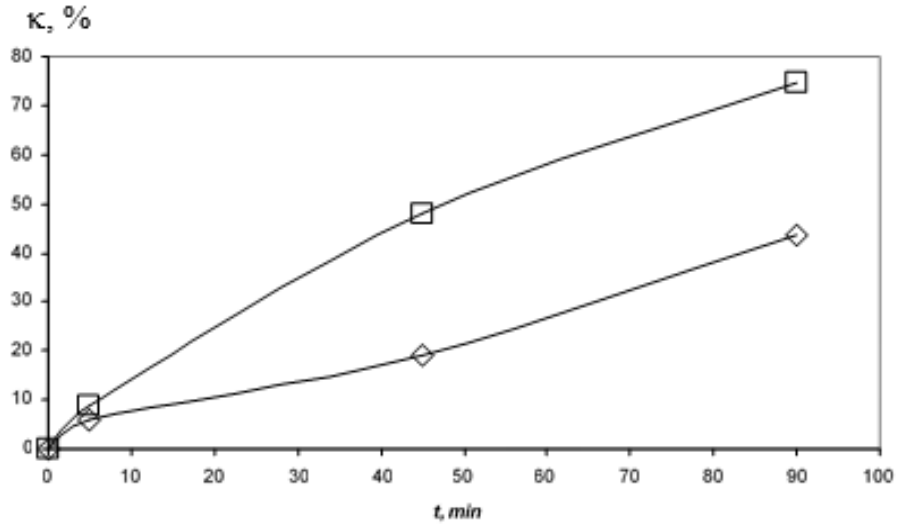

Key: κ, % *t*, min

Fig. 6. Hydrogenation of ethylbenzene at 423 K (◊) and 493 K (□): extent of conversion κ as a function of *t*; $P(H_2)$ = 2 atm.

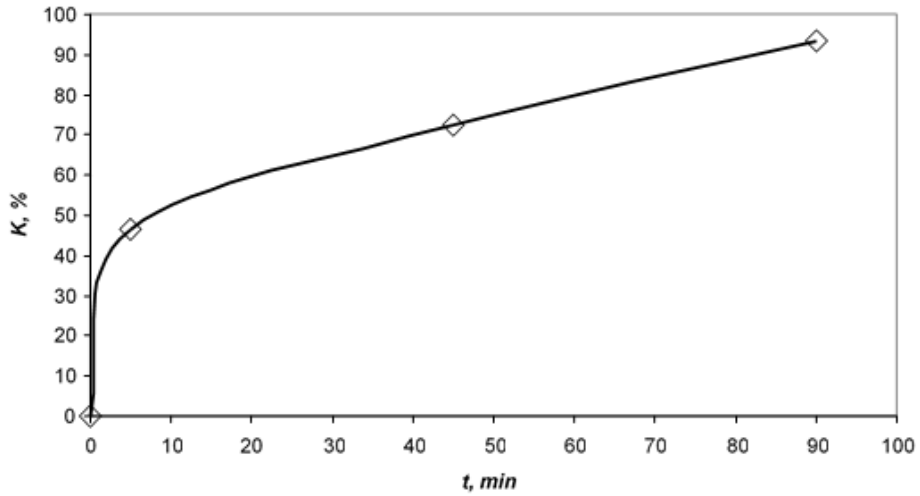

Key: κ, % *t*, min

Fig. 7. Hydrogenation of ethylbenzene at 423 K: extent of conversion κ as a function of *t*; $P(H_2)$ = 2 atm.